

# Deconstructing Prominent Bands in the Terahertz Spectra of $\text{H}_7\text{O}_3^+$ and $\text{H}_9\text{O}_4^+$ : Intermolecular Modes in Eigen Clusters

Tim K. Esser, Harald Knorke, and Knut R. Asmis\*<sup>1</sup>

Wilhelm-Ostwald-Institut für Physikalische und Theoretische Chemie, Universität Leipzig, Linnéstraße 2, 04103 Leipzig, Germany

Wieland Schöllkopf<sup>2</sup>

Fritz-Haber-Institut der Max-Planck-Gesellschaft, Faradayweg 4-6, D-14195 Berlin, Germany

Qi Yu, Chen Qu, and Joel M. Bowman\*<sup>3</sup>

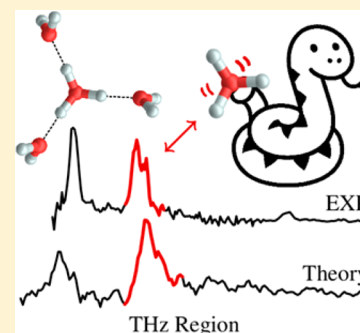
Department of Chemistry and Cherry L. Emerson Center for Scientific Computation, Emory University, Atlanta, Georgia 30322, United States

Martina Kaledin\*

Department of Chemistry and Biochemistry, Kennesaw State University, Kennesaw, Georgia 30144, United States

## Supporting Information

**ABSTRACT:** We report experimental vibrational action spectra (210–2200  $\text{cm}^{-1}$ ) and calculated IR spectra, using recent *ab initio* potential energy and dipole moment surfaces, of  $\text{H}_7\text{O}_3^+$  and  $\text{H}_9\text{O}_4^+$ . We focus on prominent far-IR bands, which postharmonic analyses show, arise from two types of intermolecular motions, i.e., hydrogen bond stretching and terminal water wagging modes, that are similar in both clusters. The good agreement between experiment and theory further validates the accuracy of the potential and dipole moment surfaces, which was used in a recent theoretical study that concluded that infrared photodissociation spectra of the cold clusters correspond to the Eigen isomer. The comparison between theory and experiment adds further confirmation of the need of postharmonic analysis for these clusters.



Recent ultrafast, infrared (IR) spectroscopic studies of excess protons in water have provided new insights into the nature of aqueous proton transfer, in general, and the role of Zundel- vs Eigen-like motifs, in particular.<sup>1,2</sup> The spectral diffusion associated with the characteristic IR absorptions of these local hydration motifs has been disentangled by gas-phase vibrational action spectroscopy on cold protonated water clusters  $\text{H}^+(\text{H}_2\text{O})_n$ , which directly correlates local distortions of the hydrogen-bonded network with vibrational frequencies in the mid- and near-IR spectral regions as a function of the displacement of the transferring proton.<sup>3</sup> However, the characteristic spectral signatures of  $\text{H}^+(\text{H}_2\text{O})_n$  clusters in the far-IR or terahertz region ( $<600 \text{ cm}^{-1}$ ), namely, intermolecular hydrogen-bond stretching and deformation modes<sup>4–7</sup> remain largely ill-characterized. IR photodissociation (IRPD) spectra in this spectral region, which require the intense and widely tunable radiation from an IR free electron laser, have only been reported for some of the larger ( $n \geq 5$ ) clusters,<sup>8–10</sup> but not for the prototypical Eigen ion,  $\text{H}_3\text{O}^+(\text{H}_2\text{O})_3$ , itself. Such spectra are reported here for the first time.

The IRPD spectra of small protonated water clusters,<sup>3,8,10–20</sup> especially the one for  $\text{H}_9\text{O}_4^+$ , have been the subject of numerous theoretical analyses,<sup>3,10,14,21–24</sup> using VPT2 theory and also “on-the-fly” *ab initio* molecular dynamics simulations of the IR spectra (both using DFT or MP2 electronic energies) and with conflicting conclusions about whether the experimental spectra are for the Eigen<sup>19,21</sup> or Zundel<sup>22</sup> isomers. Recently, two of us (Q.Y. and J.M.B.), reported many-body representations of the potential and dipole moment surfaces that are suitable for a variety of postharmonic analyses.<sup>20,23,24</sup> The representation for the potential is based on the CCSD(T)-level of theory, currently the “gold standard” method. Details of the many-body representations of the potential energy and dipole moment surfaces and validation are given elsewhere.<sup>20,24</sup> They were recently used in coupled-mode VSCF/VCI quantum calculations, employing the exact Watson Hamiltonian, of the

Received: December 23, 2017

Accepted: January 23, 2018

Published: January 23, 2018

IR spectra of  $\text{H}_7\text{O}_3^+$  and  $\text{H}_9\text{O}_4^+$  to unambiguously confirm the original assignment<sup>11</sup> that these ions exhibit Eigen-type (hydronium ion) cores (see Figure 1), i.e., they correspond to  $\text{H}_3\text{O}^+(\text{H}_2\text{O})_2$  (3E) and  $\text{H}_3\text{O}^+(\text{H}_2\text{O})_3$  (4E), respectively.<sup>20,23,24</sup>

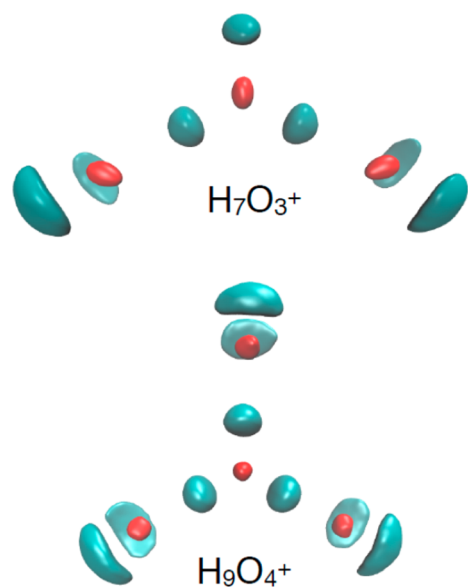


**Figure 1.** Isosurface plots of the ground vibrational wave functions of  $\text{H}^+(\text{H}_2\text{O})_3$  (3E) and  $\text{H}^+(\text{H}_2\text{O})_4$  (4E) obtained from diffusion Monte Carlo calculations. Red represents the O nuclei and turquoise the H nuclei.

Here, we present the IRPD spectra of the cryogenically cooled,  $\text{D}_2$ -tagged protonated water trimer,  $\text{H}^+(\text{H}_2\text{O})_3\text{-D}_2$ , denoted as 3H-D<sub>2</sub>, and tetramer,  $\text{H}^+(\text{H}_2\text{O})_4\text{-D}_2$  (4H-D<sub>2</sub>), in the spectral region 210–2200  $\text{cm}^{-1}$ . Tagging is required to probe the linear absorption regime and  $\text{D}_2$  was chosen to mitigate well-documented tagging issues. We conclusively assign the spectral features to hydrogen-bond stretching as well as water wagging modes based on anharmonic calculations using the high-level potential and dipole moment surfaces mentioned above. These calculations include the previous VSCF/VCI ones in the spectral range above 1000  $\text{cm}^{-1}$  and quasiclassical molecular dynamics (QCMD) calculations, described below and also in the Supporting Information (SI) for the spectral range below 1000  $\text{cm}^{-1}$ . Unfortunately, in this range the quantum approach becomes prohibitively difficult, as the large-amplitude, torsional motion of the flanking waters is poorly described by the Watson Hamiltonian. Classical MD simulations of IR spectra for low frequency modes are expected to be a substantial improvement over double harmonic oscillator (DHO) ones, as has been amply demonstrated in the literature, and also here. Addition of zero-point energy may also improve MD spectra<sup>24,25</sup> and so that is done here, but only for the intermolecular modes. This approach is essentially the well-known quasiclassical one, used in reaction dynamics calculations and so we used the term “quasiclassical” molecular dynamics above. Some analysis of the QCMD spectra is done using driven molecular dynamics (DMD), which is the mechanical analogue of the classical interaction of an external oscillating electric field with the molecular dipole. The details are given elsewhere,<sup>26–28</sup> and briefly reviewed in the SI. Finally, rigorous diffusion Monte Carlo calculations (with details given

in the SI) are done for the zero-point wave functions of 3E and 4E. These are shown, without comment, in Figure 1.

The experimental IRPD spectrum of 3H-D<sub>2</sub> in the spectral range 210 to 2200  $\text{cm}^{-1}$  is compared to the DHO, QCMD spectra and previous VSCF/VCI calculations (above 900  $\text{cm}^{-1}$ ) of (bare) 3E in Figure 2. Experimental band positions and

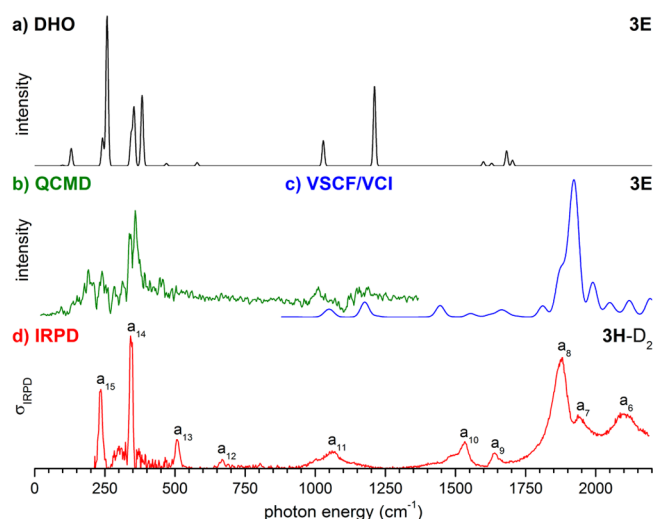


**Figure 2.** Comparison of the calculated (a) double-harmonic (DHO), (b) QCMD, and (c) VSCF/VCI vibrational spectra of 3E to the (d) experimental IRPD spectrum of 3H-D<sub>2</sub> in the spectral region from 0 to 2200  $\text{cm}^{-1}$ . See Table 1 for band positions and assignments. The calculated DHO and VSCF/VCI spectra were convoluted with Gaussian line shape functions with a fwhm width of 10 and 30  $\text{cm}^{-1}$ , respectively.

assignments, based on calculations, are listed in Table 1. The IRPD spectrum reveals (at least) 10 features, labeled with  $a_6$  to  $a_{15}$  (see ref 20 for bands  $a_1$  to  $a_5$ ). Bands  $a_6$ – $a_{11}$  agree satisfactorily with the previously published data for 3H-D<sub>2</sub> by Duong *et al.*<sup>20</sup> Minor discrepancies with respect to relative intensities are observed for  $a_6$  and the low-energy shoulder of  $a_{10}$ , which may be attributed to the slightly different conditions in the two experiments. Features  $a_{12}$  to  $a_{15}$  have not been previously reported and, in particular, the three prominent bands at 508  $\text{cm}^{-1}$  ( $a_{13}$ ), 344  $\text{cm}^{-1}$  ( $a_{14}$ ), and 234  $\text{cm}^{-1}$  ( $a_{15}$ ) correspond to the first experimental observation of transitions involving the intermolecular water modes in the protonated water trimer.

As usual, we turn to theory to assign/interpret the experimental spectra, with a specific focus on the new experimental bands. First, consider the DHO spectrum, which does have a single intense band and a higher-energy doublet in the range of experimental bands  $a_{15}$  and  $a_{14}$ . However, there are other strong bands in the DHO spectrum that are not present in experiment and vice versa. Clearly then, DHO is not reliable, or at least not globally reliable. By contrast, the QCMD spectra are in good agreement with experiment over the expected range of applicability of these spectra, and beyond that range the VSCF/VCI spectrum continues the good agreement with experiment. The QCMD spectrum was analyzed using DMD, and the results, shown in the SI, are that for the bands around 241 and 355  $\text{cm}^{-1}$  the energy absorption continues monotonically, as seen in Figure S2. This is an indication from DMD that these are intense bands, in agreement with the QCMD results (and also the

**Table 1. Experimental IRPD Band Positions (in  $\text{cm}^{-1}$ ) of  $3\text{H-D}_2$ , Computed Harmonic (HO), VSCF/VCI, and QCMD Vibrational Wavenumbers (in  $\text{cm}^{-1}$ ) of  $3\text{E}$  and Assignments**

label	IRPD	IRPD <sup>a</sup>	HO	VSCF/VCI <sup>a</sup>	QCMD	assignment <sup>b</sup>
a <sub>6</sub>	2100	2109		2098–2246		low freq modes + H <sub>3</sub> O <sup>+</sup> bend + IHB antisym. stretch, H <sub>3</sub> O <sup>+</sup> frust. rotation + H <sub>2</sub> O bend + IHB sym. stretch
a <sub>7</sub>	1942	1943	2692	2034		2ν H <sub>3</sub> O <sup>+</sup> wag + IHB sym. stretch
a <sub>8</sub>	1875	1878	2518	1910–1976		IHB antisym stretch, H <sub>3</sub> O <sup>+</sup> frust. rotation + H <sub>3</sub> O <sup>+</sup> umbrella + IHB antisym. stretch
a <sub>9</sub>	1640	1639	1721,1743	1688,1701		H <sub>3</sub> O <sup>+</sup> bend
a <sub>10</sub>	1533	1534	1636,1666	1477		H <sub>2</sub> O bend + IHB antisym. stretch
a <sub>11</sub>	1060	1059	1240	1202	1176	H <sub>3</sub> O <sup>+</sup> umbrella
a <sub>12</sub>	668		1051	1081	1015	H <sub>3</sub> O <sup>+</sup> wag
a <sub>13</sub>	508		593			H <sub>3</sub> O <sup>+</sup> frust. rotation
a <sub>14</sub>	344		479		456	comb of low freq modes
			390			antisym. HB-stretch (H <sub>3</sub> O <sup>+</sup> rattle)
			362		355	sym. HB-stretch
			351			H <sub>2</sub> O rock
a <sub>15</sub>	234		264		241	H <sub>2</sub> O wag
			247			

<sup>a</sup>From ref 20. <sup>b</sup>Band assignments for a<sub>6</sub> to a<sub>11</sub> from ref 20.

DHO ones) and experiment. By contrast, the energy absorbed stops for the two intense DHO bands at 1051 and 1240  $\text{cm}^{-1}$  (see Table 1), indicating that these are in fact weak absorbers. This agrees with the QCMD spectrum and also experiment; however, not with the DHO results. Finally, we note that there are no DHO peaks in the spectral range 1750–2200  $\text{cm}^{-1}$ , in contrast to experimental and VSCF/VCI spectra.

The experimental IRPD spectrum of  $4\text{H-D}_2$  in the spectral range from 210 to 2200  $\text{cm}^{-1}$  is compared to the DHO and QCMD spectra of bare  $4\text{E}$  in Figure 3. Band positions and assignments are listed in Table 2. The IRPD spectrum shows eight bands (a<sub>10</sub>'–a<sub>17</sub>') in total, with two characteristic and intense IR bands and a weaker feature in the far IR region at 316  $\text{cm}^{-1}$  (a<sub>16</sub>'), 236  $\text{cm}^{-1}$  (a<sub>17</sub>'), and 503  $\text{cm}^{-1}$  (a<sub>15</sub>'). Bands a<sub>10</sub>'–a<sub>14</sub>' agree satisfactorily with the previously reported spectrum of  $4\text{H-D}_2$  by Wolke *et al.*<sup>3</sup> Minor discrepancies

(–10  $\text{cm}^{-1}$ ) with respect to the position of the band maximum of a<sub>10</sub>' and of a<sub>11</sub>' are observed and due to slightly different band profiles.

We first discuss the assignments of the prominent experimental bands labeled a<sub>17</sub>'/a<sub>15</sub> and a<sub>16</sub>'/a<sub>14</sub>. By examining trajectories that correspond to these, the intensity of bands a<sub>17</sub>'/a<sub>15</sub> is due to mainly “wagging” motion of the flanking H<sub>2</sub>O molecules and for bands a<sub>16</sub>'/a<sub>14</sub> it is the embedded H<sub>3</sub>O<sup>+</sup> hydrogen bond stretching (or “H<sub>3</sub>O<sup>+</sup> rattle”) mode that is the dominant motion. In both cases, there is evidently a large change in the dipole moment. This is worth investigating in detail, and this is done in Figure 4, where the components of the full dipole moment are plotted along with the component from the above many-body representation of the dipole moment, as a function of the corresponding intermolecular normal mode corresponding closest to the quasiclassical motion. Even though this normal mode may not be as accurate a description of the QC motion, it suffices for this qualitative explanation of the intensity. In the upper panel, for the wagging motion, we see that the sum of the 1-body water and 2-body water dipole tracks the full dipole nearly exactly as a function of Q. The magnitude is less but the derivative is nearly identical and so we are safe in assigning the intensity to the change in the sum of the water monomer dipole moments. The lower panel shows a more complex picture for the dipole moment of the H<sub>3</sub>O<sup>+</sup> hydrogen bond stretching mode; however, it is clear that change in the 1-body hydronium dipole plus the 2-body hydronium water dipole moment are the main contributors to the intensity. This picture is not as obvious as the one for the wagging of the flanking water; however, it results from coupling of the hydronium and the water intermolecular modes, in this case the H<sub>3</sub>O<sup>+</sup> hydrogen bond stretch mode.

Comparison of the intense bands below 800  $\text{cm}^{-1}$  with those observed in-between 800 and 2100  $\text{cm}^{-1}$  in the IRPD spectra of  $3\text{H-D}_2$  and  $4\text{H-D}_2$  reveals that the lower frequency bands are considerably narrower, exhibiting fwhm widths of less than ~15  $\text{cm}^{-1}$ , similar (a) to the bands found in the free O–H stretching region<sup>3,20</sup> as well as (b) to the corresponding bands in the spectra of  $5\text{H-D}_2$  and  $6\text{H-H}_2$ .<sup>8,10</sup> The QCMD results predict broader band profiles for a<sub>13</sub>/a<sub>14</sub> ( $3\text{E}$ ) and a<sub>16</sub>'/a<sub>17</sub>' ( $4\text{E}$ ), but these bands from theory do show some sensitivity to the energy of the trajectories; this is typical of MD approaches. We find no

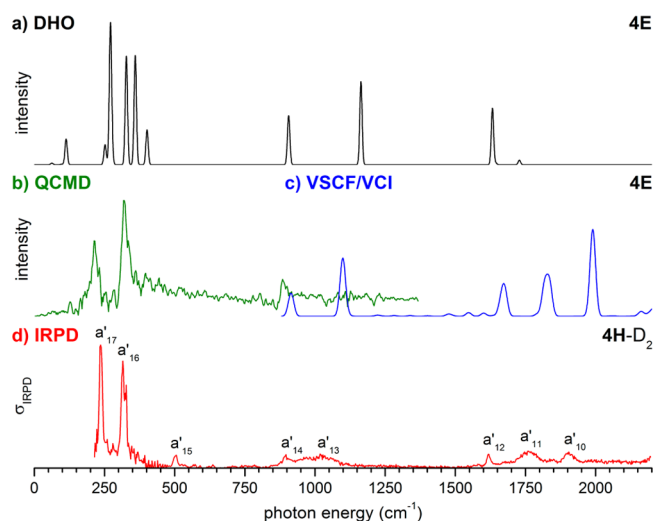


**Figure 3.** Comparison of the calculated (a) double-harmonic (DHO), (b) QCMD and (c) VSCF/VCI vibrational spectra of  $4\text{E}$  to the (d) experimental IRPD spectrum of  $4\text{H-D}_2$  in the spectral region from 0 to 2200  $\text{cm}^{-1}$ . See Table 2 for band positions and assignments. The calculated DHO and VSCF/VCI spectra were convoluted with Gaussian line shape functions with a fwhm width of 10 and 30  $\text{cm}^{-1}$ , respectively.

**Table 2. Experimental IRPD Band Positions (in  $\text{cm}^{-1}$ ) of 4H-D<sub>2</sub>, Computed Harmonic (HO), VSCF/VCI, and QCMD Vibrational Wavenumbers (in  $\text{cm}^{-1}$ ) of 4E and Assignments**

label	IRPD	IRPD <sup>a</sup>	HO	VSCF/VCI <sup>b</sup>	QCMD	assignment <sup>c</sup>
a <sub>10</sub> '	1898	1909		2033		H <sub>3</sub> O <sup>+</sup> umbrella + H <sub>3</sub> O <sup>+</sup> wag
a <sub>11</sub> '	1760	1770		1859,1877		overtone H <sub>3</sub> O <sup>+</sup> wag, comb 2 H <sub>3</sub> O <sup>+</sup> wag
a <sub>12</sub> '	1615	1615	1669–1768	1712		H <sub>3</sub> O <sup>+</sup> and H <sub>2</sub> O bends
a <sub>13</sub> '	1014		1190	1124	1154	H <sub>3</sub> O <sup>+</sup> umbrella
a <sub>14</sub> '	894		928	937	910	H <sub>3</sub> O <sup>+</sup> wag
a <sub>15</sub> '	503					comb of low freq modes
a <sub>16</sub> '	316		335–411		331	antisym. HB - stretch (H <sub>3</sub> O <sup>+</sup> rattle)
a <sub>17</sub> '	236		258–284		216	sym. HB - stretch H <sub>2</sub> O wag

<sup>a</sup>From ref 3. <sup>b</sup>From refs 23 and 24. <sup>c</sup>Band assignments for a<sub>10</sub>' to a<sub>14</sub>' from refs 3, 23, and 24.

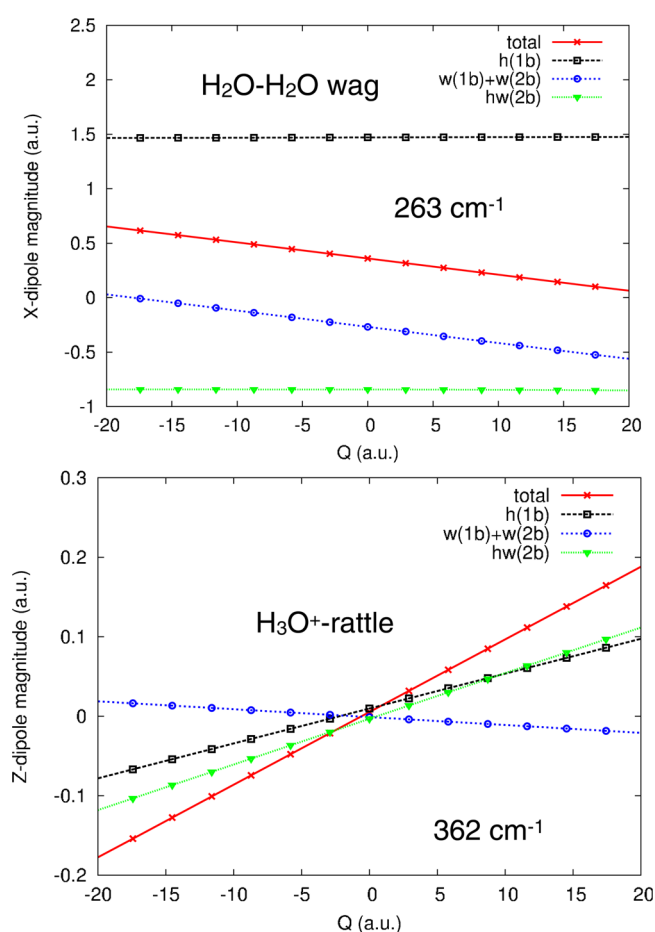


**Figure 4.** Normal mode dependence of the major component of the dipole moment for bands a<sub>15</sub> and a<sub>14</sub> of 3E. See text for details.

evidence that this narrowness originates from multiphoton absorption effects. We employed modest laser pulse energies (<1 mJ below 500  $\text{cm}^{-1}$ ) and estimates of the dissociation limit, when zero-point and internal energies are considered, support that single photon photodissociation is feasible. Tagging effects should also not alter the band widths dramatically, but probably do contribute to the deviations regarding the band positions and relative intensities. Tables S3 and S4, which contain the harmonic MP2 frequencies with and without the D<sub>2</sub> tag, can be consulted for guidance on the effect of tagging. However, because the spectra in the THz region are highly anharmonic and coupled, the numerical values of the shifts should not be taken as accurate. Summarizing, the intermolecular stretching

and wagging frequencies appear surprisingly insensitive to the inherent floppiness of these hydrogen-bonded ions.

Finally, it is of interest to discuss how the present values for the IR-active low-frequency modes compare to those in larger protonated water clusters and in solution (see Table 3). The

**Table 3. Evolution of the Band Positions (in  $\text{cm}^{-1}$ ) of the IR-Active Hydrogen-Bond Stretching Vibrations Associated with the H<sub>3</sub>O<sup>+</sup> Core in the Experimental IR Spectra of Protonated Water Clusters H<sup>+</sup>(H<sub>2</sub>O)<sub>n</sub> with Cluster Size n up to the Condensed Phase Limit**

n	experiment
3	344
4	316
5 <sup>a</sup>	405/298
6 <sup>b</sup>	373/279
21 <sup>c</sup>	341
∞ <sup>d</sup>	~340

<sup>a</sup>Ref 10. <sup>b</sup>Ref 8. <sup>c</sup>Ref 9. <sup>d</sup>Ref 7.

Eigen ion 4E exhibits 12 vibrational normal modes in the terahertz spectral region (<600  $\text{cm}^{-1}$ ), which correspond to frustrated translations and rotations of the flanking water molecules. These are, in order of decreasing frequency, the three hydrogen bond stretching, three water wagging, three water rocking, and three hydrogen bond deformation (bending) modes. Each set consists of a symmetric and a doubly degenerate antisymmetric combination, of which only the antisymmetric hydrogen bond stretching and water wagging modes carry significant IR intensity. These are observed at 316 and 236  $\text{cm}^{-1}$ , respectively, in the spectrum of 4H-D<sub>2</sub>. Removal of one of the flanking waters leads to 3E with only single antisymmetric stretching and wagging modes (3H-D<sub>2</sub>: 344 and 234  $\text{cm}^{-1}$ , respectively).

While it proves difficult to unambiguously identify the wagging modes of the flanking water molecules in larger water clusters, due to their delocalized nature over an increased number of water molecules, the respective hydrogen-bond stretching modes involving the embedded H<sub>3</sub>O<sup>+</sup> can be traced all the way to the solution phase data (see Table 3). The asymmetrically solvated H<sub>3</sub>O<sup>+</sup> in 5E and 6E results in a splitting of the IR-active (antisymmetric) hydrogen bond stretches, one that is blue-shifted in the spectra of 5H-D<sub>2</sub> (405  $\text{cm}^{-1}$ )<sup>10</sup> and 6H-D<sub>2</sub> (373  $\text{cm}^{-1}$ )<sup>8</sup> and another that is red-shifted (5H-D<sub>2</sub>: 298  $\text{cm}^{-1}$ , 6H-D<sub>2</sub>: 279  $\text{cm}^{-1}$ ), with respect to their position in the 4H-D<sub>2</sub> spectrum. This yields mean frequencies for these modes of 351  $\text{cm}^{-1}$  (n = 5) and 326  $\text{cm}^{-1}$

( $n = 6$ ). At  $n = 21$ ,  $\text{H}_3\text{O}^+$  is more symmetrically solvated again, and the  $2\text{H-D}_2$  spectrum<sup>9</sup> features a single, prominent broad IR-active band at  $341\text{ cm}^{-1}$ , very close to the solution value of  $340\text{ cm}^{-1}$ .<sup>7</sup> Summarizing, the *mean* frequencies of the IR-active hydrogen-bond stretching modes involving the hydronium core in protonated water clusters lie in a narrow spectral window ( $\sim 310\text{--}360\text{ cm}^{-1}$ ) and seem to have converged close to the bulk value of  $340\text{ cm}^{-1}$  ( $n = \infty$ ) already for  $n = 21$ , suggesting a rather localized nature of these modes.

## ■ EXPERIMENTAL DETAILS

IRPD experiments are performed using a 6 K ion-trap triple mass spectrometer described previously.<sup>29</sup> In brief, protonated water clusters are generated in a nano-electrospray source from a 10 mM solution of sulfuric acid in a 1:1 water/methanol mixture, thermalized at room temperature in a gas-filled radio frequency (RF) ion-guide, mass-selected using a quadrupole mass filter, and focused in a RF ring-electrode ion-trap. The trap is continuously filled with  $\text{D}_2$  buffer gas, cooled with a closed-cycle He cryostat, and held at temperatures between 13 to 15 K. Many collisions of the trapped ions with the buffer gas provide gentle cooling of the internal degrees of freedom close to the ambient temperature. At sufficiently low ion-trap temperatures, ion-messenger complexes are formed via three body collisions.<sup>30,31</sup> All ions are extracted either every 100 or 200 ms, depending on the lasers used, and focused both temporally and spatially into the center of the extraction region of an orthogonally mounted reflectron time-of-flight (TOF) tandem photofragmentation mass spectrometer. Here, the ions are irradiated with a counter-propagating IR laser pulse produced either by the free electron laser FHI FEL<sup>32</sup> ( $210\text{--}1200\text{ cm}^{-1}$ ) at the Fritz Haber Institute in Berlin or an OPO/OPA/AgGaSe<sub>2</sub> IR laser system<sup>33</sup> ( $700\text{--}2000\text{ cm}^{-1}$ ). All parent and photofragment ions are then accelerated toward an MCP detector and monitored simultaneously as the laser wavelength is scanned. The photodissociation cross section  $\sigma_{\text{IRPD}}$  is determined as described previously.<sup>29,34</sup> The individual IRPD spectra using the two laser systems are then scaled in intensity such that the intensity of common peaks in the overlapping region ( $700\text{--}1200\text{ cm}^{-1}$ ) match, in order to correct for changes in laser beam/ion cloud overlap (see Figures S5 and S6).

The FHI FEL is operated at 5 Hz with a bandwidth of approximately  $3\text{ cm}^{-1}$  and an average power of 50 mJ per macropulse (laser pulse). IR pulse energies are reduced by attenuators to less than 6 mJ ( $<1\text{ mJ}$  below  $500\text{ cm}^{-1}$ ) to avoid saturation. IRPD spectra are recorded by averaging over 50–75 TOF mass spectra per wavelength step and scanning the wavelength of the laser pulse.

The OPO/OPA laser system is operated at 10 Hz with a bandwidth of approximately  $3\text{ cm}^{-1}$  and an average power of 1–1.5 mJ per laser pulse. IRPD spectra are measured by continuously scanning the laser wavelength, which is monitored online using a HighFinesse WS6–600 wavelength meter, with a scan speed such that an averaged TOF mass spectrum (over 100 laser shots) is obtained every  $2\text{ cm}^{-1}$ . Typically, at least three scans are measured.

## ■ COMPUTATIONAL DETAILS

The IR spectra of  $\text{H}_7\text{O}_3^+$  and  $\text{H}_9\text{O}_4^+$  in the region 0 to  $1200\text{ cm}^{-1}$  were calculated using a quasiclassical molecular dynamics (QCMD) approach to obtain the dipole–dipole correlation function, the Fourier transform of which provides the IR

spectrum. The QCMD approach we take is a minor modification of the procedure described by Van-Oanh et al.,<sup>25</sup> where zero-point energy is given initially to each normal mode of a molecule. This approach is widely used in reaction dynamics, where it is referred to as the quasiclassical approach, and so we use that terminology here. It is well-known that this approach suffers from “zero-point leak”, because it is actually an approximate semiclassical quantization procedure and thus mode–mode energy transfer can occur. (This “leak” would in principle be eliminated if exact semiclassical quantization of the zero-point state was done.) The energy transfer from high-frequency intramolecular modes to low-frequency intermolecular ones can result in rapid dissociation of the molecule/complex. To mitigate this rapid dissociation, we apply the approximate quasiclassical quantization to intermolecular modes only and give zero energy initially to the intramolecular modes.

One hundred trajectories were performed for each complex. The initial conditions were obtained by random sampling of the harmonic normal-mode phase space, with harmonic zero-point energy given to the intermolecular modes. Each trajectory was propagated for 12 ps and the standard dipole–dipole correlation function was obtained for each, then averaged over the set of trajectories, and finally Fourier transformed to obtain the spectra. No smoothing of the spectra was done.

Additional details of the computations, especially for the driven molecular dynamics ones are given in the SI.

## ■ ASSOCIATED CONTENT

### Supporting Information

The Supporting Information is available free of charge on the ACS Publications website at DOI: [10.1021/acs.jpcllett.7b03395](https://doi.org/10.1021/acs.jpcllett.7b03395).

This contains the harmonic frequencies of the bare and  $\text{D}_2$ -tagged ions, some details of the driven molecular dynamics calculations, the conventional NVE MD IR spectra, diffusion Monte Carlo calculations, and details regarding the laser pulse energies used to measure the IRPD spectra (PDF)

## ■ AUTHOR INFORMATION

### Corresponding Authors

\*E-mail: [knut.asmis@uni-leipzig.de](mailto:knut.asmis@uni-leipzig.de).

\*E-mail: [jmbowma@emory.edu](mailto:jmbowma@emory.edu).

\*E-mail: [mkaledin@kennesaw.edu](mailto:mkaledin@kennesaw.edu).

### ORCID

Knut R. Asmis: 0000-0001-6297-5856

Wieland Schöllkopf: 0000-0003-0564-203X

Joel M. Bowman: 0000-0001-9692-2672

### Notes

The authors declare no competing financial interest.

## ■ ACKNOWLEDGMENTS

T.E., H.K., and K.R.A. gratefully acknowledge funding by the German Research Foundation (DFG) as part of the individual research grant AS133/3-1 and instrumental support by Nadja Heine, Matias Fagiani, and Sandy Gewinner. Q.Y. and J.M.B. thank the National Science Foundation (CHE-1463552) for financial support. M.K. thanks Advanced Computer Services at Kennesaw State University for providing high performance computer system.

## REFERENCES

- (1) Thamer, M.; De Marco, L.; Ramasesha, K.; Mandal, A.; Tokmakoff, A. Ultrafast 2D IR spectroscopy of the excess proton in liquid water. *Science* **2015**, *350*, 78–82.
- (2) Dahms, F.; Fingerhut, B. P.; Nibbering, E. T. J.; Pines, E.; Elsaesser, T. Large-amplitude transfer motion of hydrated excess protons mapped by ultrafast 2D IR spectroscopy. *Science* **2017**, *357*, 491–494.
- (3) Wolke, C. T.; Fournier, J. A.; Dzugan, L. C.; Fagiani, M. R.; Odbadrakh, T. T.; Knorke, H.; Jordan, K. D.; McCoy, A. B.; Asmis, K. R.; Johnson, M. A. Spectroscopic snapshots of the proton-transfer mechanism in water. *Science* **2016**, *354*, 1131–1135.
- (4) Braly, L. B.; Liu, K.; Brown, M. G.; Keutsch, F. N.; Fellers, R. S.; Saykally, R. J. Terahertz laser spectroscopy of the water dimer intermolecular vibrations. II.  $(\text{H}_2\text{O})_2$ . *J. Chem. Phys.* **2000**, *112*, 10314–10326.
- (5) Keutsch, F. N.; Saykally, R. J. Water clusters: Untangling the mysteries of the liquid, one molecule at a time. *Proc. Natl. Acad. Sci. U. S. A.* **2001**, *98*, 10533–10540.
- (6) Saykally, R. J.; Wales, D. J. Pinning Down the Water Hexamer. *Science* **2012**, *336*, 814–815.
- (7) Decka, D.; Schwaab, G.; Havenith, M. A THz/FTIR fingerprint of the solvated proton: evidence for Eigen structure and Zundel dynamics. *Phys. Chem. Chem. Phys.* **2015**, *17*, 11898–11907.
- (8) Heine, N.; Fagiani, M. R.; Rossi, M.; Wende, T.; Berden, G.; Blum, V.; Asmis, K. R. Isomer-selective detection of hydrogen-bond vibrations in the protonated water hexamer. *J. Am. Chem. Soc.* **2013**, *135*, 8266–8273.
- (9) Fournier, J. A.; Wolke, C. T.; Johnson, C. J.; Johnson, M. A.; Heine, N.; Gewinner, S.; Schöllkopf, W.; Esser, T. K.; Fagiani, M. R.; Knorke, H.; Asmis, K. R. Site-specific vibrational spectral signatures of water molecules in the magic  $\text{H}_3\text{O}^+(\text{H}_2\text{O})_{20}$  and  $\text{Cs}^+(\text{H}_2\text{O})_{20}$  clusters. *Proc. Natl. Acad. Sci. U. S. A.* **2014**, *111*, 18132–18137.
- (10) Fagiani, M. R.; Knorke, H.; Esser, T. K.; Heine, N.; Wolke, C. T.; Gewinner, S.; Schöllkopf, W.; Gaigeot, M.-P.; Spezia, R.; Johnson, M. A.; Asmis, K. R. Gas phase vibrational spectroscopy of the protonated water pentamer: the role of isomers and nuclear quantum effects. *Phys. Chem. Chem. Phys.* **2016**, *18*, 26743–26754.
- (11) Okumura, M.; Yeh, L. I.; Myers, J. D.; Lee, Y. T. Infrared spectra of the cluster ions  $\text{H}_7\text{O}_3^+\text{H}_2$  and  $\text{H}_9\text{O}_4^+\text{H}_2$ . *J. Chem. Phys.* **1986**, *85*, 2328–9.
- (12) Jiang, J. C.; Wang, Y. S.; Chang, H. C.; Lin, S. H.; Lee, Y. T.; Niedner-Schatteburg, G.; Chang, H. C. Infrared spectra of  $\text{H}^+(\text{H}_2\text{O})_{5-8}$  clusters: Evidence for symmetric proton hydration. *J. Am. Chem. Soc.* **2000**, *122*, 1398–1410.
- (13) Asmis, K. R.; Pivonka, N. L.; Santambrogio, G.; Brümmer, M.; Kaposta, C.; Neumark, D. M.; Wöste, L. Gas-phase infrared spectrum of the protonated water dimer. *Science* **2003**, *299*, 1375–1377.
- (14) Headrick, J. M.; Diken, E. G.; Walters, R. S.; Hammer, N. I.; Christie, R. A.; Cui, J.; Myshakin, E. M.; Duncan, M. A.; Johnson, M. A.; Jordan, K. D. Spectral signatures of hydrated proton vibrations in water clusters. *Science* **2005**, *308*, 1765–1769.
- (15) Douberly, G. E.; Walters, R. S.; Cui, J.; Jordan, K. D.; Duncan, M. A. Infrared spectroscopy of small protonated water clusters,  $\text{H}^+(\text{H}_2\text{O})_n$  ( $n = 2-5$ ): Isomers, argon tagging, and deuteration. *J. Phys. Chem. A* **2010**, *114*, 4570–4579.
- (16) Mizuse, K.; Fujii, A. Infrared photodissociation spectroscopy of  $\text{H}^+(\text{H}_2\text{O})_6\text{-M}_m$  ( $M = \text{Ne, Ar, Kr, Xe, H}_2, \text{N}_2, \text{and CH}_4$ ): messenger-dependent balance between  $\text{H}_3\text{O}^+$  and  $\text{H}_5\text{O}_2^+$  core isomers. *Phys. Chem. Chem. Phys.* **2011**, *13*, 7129–7135.
- (17) Mizuse, K.; Fujii, A. Tuning of the internal energy and isomer distribution in small protonated water clusters  $\text{H}^+(\text{H}_2\text{O})_{4-8}$ : An application of the inert gas messenger technique. *J. Phys. Chem. A* **2012**, *116*, 4868–4877.
- (18) Heine, N.; Fagiani, M. R.; Asmis, K. R. Disentangling the contribution of multiple isomers to the infrared spectrum of the protonated water heptamer. *J. Phys. Chem. Lett.* **2015**, *6*, 2298–2304.
- (19) Fournier, J. A.; Wolke, C. T.; Johnson, M. A.; Odbadrakh, T. T.; Jordan, K. D.; Kathmann, S. M.; Xantheas, S. S. Snapshots of proton accommodation at a microscopic water surface: Understanding the vibrational spectral signatures of the charge defect in cryogenically cooled  $\text{H}^+(\text{H}_2\text{O})_{n=2-28}$  clusters. *J. Phys. Chem. A* **2015**, *119*, 9425–9440.
- (20) Duong, C. H.; Gorlova, O.; Yang, N.; Kelleher, P. J.; Johnson, M. A.; McCoy, A. B.; Yu, Q.; Bowman, J. M. Disentangling the complex vibrational spectrum of the protonated water trimer,  $\text{H}^+(\text{H}_2\text{O})_3$ , with two-color IR-IR photodissociation of the bare ion and anharmonic VSCF/VCI theory. *J. Phys. Chem. Lett.* **2017**, *8*, 3782–3789.
- (21) Yagi, K.; Thomsen, B. Infrared spectra of protonated water clusters,  $\text{H}^+(\text{H}_2\text{O})_4$ , in Eigen and Zundel forms studied by vibrational quasi-degenerate perturbation theory. *J. Phys. Chem. A* **2017**, *121*, 2386–2398.
- (22) Wang, H.; Agmon, N. Reinvestigation of the infrared spectrum of the gas-phase protonated water tetramer. *J. Phys. Chem. A* **2017**, *121*, 3056–3070.
- (23) Yu, Q.; Bowman, J. M. Communication: VSCF/VCI vibrational spectroscopy of  $\text{H}_7\text{O}_3^+$  and  $\text{H}_9\text{O}_4^+$  using high-level, many-body potential energy surface and dipole moment surfaces. *J. Chem. Phys.* **2017**, *146*, 121102.
- (24) Yu, Q.; Bowman, J. M. High-level quantum calculations of the IR spectra of the Eigen, Zundel, and Ring isomers of  $\text{H}^+(\text{H}_2\text{O})_4$  find a single match to experiment. *J. Am. Chem. Soc.* **2017**, *139*, 10984–10987.
- (25) Van-Oanh, N. T.; Falvo, C.; Calvo, F.; Lauvergnat, D.; Basire, M.; Gaigeot, M. P.; Parneix, P. Improving anharmonic infrared spectra using semiclassically prepared molecular dynamics simulations. *Phys. Chem. Chem. Phys.* **2012**, *14*, 2381–2390.
- (26) Bowman, J. M.; Zhang, X. B.; Brown, A. Normal-mode analysis without the Hessian: A driven molecular-dynamics approach. *J. Chem. Phys.* **2003**, *119*, 646–650.
- (27) Kaledin, M.; Brown, A.; Kaledin, A. L.; Bowman, J. M. Normal mode analysis using the driven molecular dynamics method. II. An application to biological macromolecules. *J. Chem. Phys.* **2004**, *121*, 5646–5653.
- (28) Kaledin, M.; Kaledin, A. L.; Bowman, J. M. Vibrational analysis of the  $\text{H}_5\text{O}_2^+$  infrared spectrum using molecular and driven molecular dynamics. *J. Phys. Chem. A* **2006**, *110*, 2933–2939.
- (29) Heine, N.; Asmis, K. R. Cryogenic ion trap vibrational spectroscopy of hydrogen-bonded clusters relevant to atmospheric chemistry. *Int. Rev. Phys. Chem.* **2015**, *34*, 1–34.
- (30) Brümmer, M.; Kaposta, C.; Santambrogio, G.; Asmis, K. R. Formation and photodepletion of cluster ion-messenger atom complexes in a cold ion trap: Infrared spectroscopy of  $\text{VO}^+$ ,  $\text{VO}_2^+$ , and  $\text{VO}_3^+$ . *J. Chem. Phys.* **2003**, *119*, 12700–12703.
- (31) Goebbert, D. J.; Wende, T.; Bergmann, R.; Meijer, G.; Asmis, K. R. Messenger-Tagging electrosprayed ions: Vibrational spectroscopy of suberate dianions. *J. Phys. Chem. A* **2009**, *113*, 5874–5880.
- (32) Schöllkopf, W.; Gewinner, S.; Junkes, H.; Paarmann, A.; von Helden, G.; Bluem, H.; Todd, A. M. M. The new IR and THz FEL facility at the Fritz Haber Institute in Berlin. *Proc. SPIE* **2015**, *9512*, 95121L.
- (33) Bosenberg, W. R.; Guyer, D. R. Broadly tunable, single-frequency optical parametric frequency conversion system. *J. Opt. Soc. Am. B* **1993**, *10*, 1716–22.
- (34) Heine, N.; Asmis, K. R. Cryogenic ion trap vibrational spectroscopy of hydrogen-bonded clusters relevant to atmospheric chemistry (vol. 34, pg. 1, 2015). *Int. Rev. Phys. Chem.* **2016**, *35*, 507–507.